A Visual Dual-Aptamer Logic Gate for Sensitive Discrimination of Prion Diseases-Associated Isoform with Reusable Magnetic Microparticles and Fluorescence Quantum Dots

Sai Jin Xiao[1,2], Ping Ping Hu[3], Li Qiang Chen[3], Shu Jun Zhen[1], Li Peng[3], Yuan Fang Li[1], Cheng Zhi Huang[1,4]*

1 Education Ministry Key Laboratory on Luminescence and Real-Time Analysis, College of Chemistry and Chemical Engineering, Southwest University, Chongqing, China, 2 Jiangxi Key Laboratory of Mass Spectrometry and Instrumentation, Department of Applied Chemistry, East China Institute of Technology, Nanchang, Jiangxi Province, China, 3 College of Life Science, Southwest University, Chongqing, China, 4 College of Pharmaceutical Sciences, Southwest University, Chongqing, China

Abstract

Molecular logic gates, which have attracted increasing research interest and are crucial for the development of molecular-scale computers, simplify the results of measurements and detections, leaving the diagnosis of disease either "yes" or "no". Prion diseases are a group of fatal neurodegenerative disorders that happen in human and animals. The main problem with a diagnosis of prion diseases is how to sensitively and selectively discriminate and detection of the minute amount of PrP^{Res} in biological samples. Our previous work had demonstrated that dual-aptamer strategy could achieve highly sensitive and selective discrimination and detection of prion protein (cellular prion protein, PrP^{C}, and the diseases associated isoform, PrP^{Res}) in serum and brain. Inspired by the advantages of molecular logic gate, we further conceived a new concept for dual-aptamer logic gate that responds to two chemical input signals (PrP^{C} or PrP^{Res} and Gdn-HCl) and generates a change in fluorescence intensity as the output signal. It was found that PrP^{Res} performs the "OR" logic operation while PrP^{C} performs "XOR" logic operation when they get through the gate consisted of aptamer modified reusable magnetic microparticles (MMPs-Apt1) and quantum dots (QDs-Apt2). The dual-aptamer logic gate simplifies the discrimination results of PrP^{Res}, leaving the detection of PrP^{Res} either "yes" or "no". The development of OR logic gate based on dual-aptamer strategy and two chemical input signals (PrP^{Res} and Gdn-HCl) is an important step toward the design of prion diseases diagnosis and therapy systems.

Competing Interests: The authors have declared that no competing interests exist.

* E-mail: chengzhi@swu.edu.cn

Introduction

Logic gate, an original concept of a programmable computer, performs a logical operation on one or more logic inputs and produces a single logic output. For example, the OR logic gate combines input 1 (i_1) and input 2 (i_2), and results in the output of 1 when i_1 and/or i_2 is 1, while XOR logic gate is a combinatorial logic gates with the output of 1 when i_1 is not equal to i_2. By analogy, molecular logic gates, which have attracted increasing research interest, perform logical operation inputs resulting from chemical or biological processes and generate a single logic output such as spectral or electrochemical signal. Several prototypes on the basis of DNA [1–2], RNA [3], and deoxyribozymes [4], biochemical pathways in living cell and organic molecules [5–7] have been designed up to now. It can be seen that the molecular logical gates simplify the results of measurements and detections, leaving the diagnosis of disease either "yes" or "no", or the detection of analytes in samples either "have" or "none".

Prion diseases, a group of fatal neurodegenerative disorders, happens in human and animals. The emergence of vCJD and its linkages to BSE triggers the researchers to develop methods for prion diseases diagnosis at the pre-symptomatic stage [8,9]. As the pathological form of prion protein, PrP^{Res}, is abundant only at the late stages in brain, the main problem for prion diseases diagnosis at pre-symptomatic stage is how to detect the minute quantities of PrP^{Res} in complex biological systems. Early methods such as western blot assays and enzyme-linked immunosorbent assays (ELISAs) are insufficient sensitive. Thus researchers attempted to use conformational antibodies with various spectroscopic techniques to improve the sensitivity [10–13], however, the worldwide application of such methods is limited by the usefulness and specificity of antibodies or expensive and sophisticated equipment.

With the purpose of addressing the limitations mentioned above, we developed a sensitive and selective PrP^{Res} discrimination and detection assay taking the advantages of aptamers since more and more aptamers against prion protein were selected
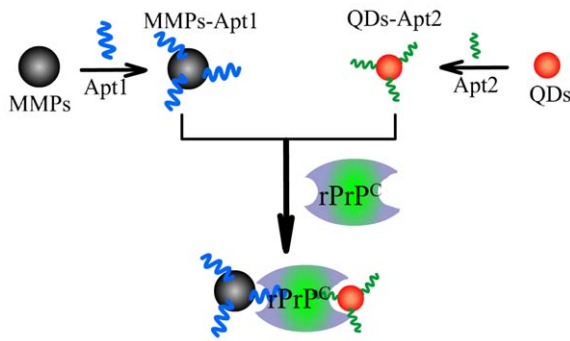
Figure 1. Schematic representation of dual-aptamer strategy for prion proteins detection.
doi:10.1371/journal.pone.0053935.g001

based on the known capacity of PrP to bind nucleic acids [14–16]. Aptamers have been applied in protein detection [17,18], diseases diagnosis [19,20], cell imaging and tracking [21,22] ect. owing to the advantages of exceptional stability, easy manipulation and reproducibility, non-toxic and diagnostic potential. Previous aptamer-based assays mainly adopted single aptamer strategy, however the sensitivity and specificity of such assay is usually insufficient for target detection especially when they applied in complex biological samples [23,24]. Our pioneer work have also demonstrated that highly sensitive and selective discrimination and detection of PrP^{Res} in serum and brain homogenate could be achieved without sample pretreatment by dual-aptamer strategy, and the results showed that the sensitivity of dual aptamer-based assay is 1000 folds higher than that of antibody-based method [25]. Inspired by the advantages of molecular logic gate and dual-aptamer strategy, we further concieved a new concept for dual-aptamer logic gate that responds to two chemical input signals (PrP^C or PrP^{Res} and Gdn-HCl) and generates a change in fluorescence intensity as the output signal. It is found that PrP^{Res} performs OR logic gate operation and PrP^C performs XOR logic gate operation on the gate consisted of aptamers modified magnetic microparticles (MMPs-Apt1) and quantum dots (QDs-Apt2). The development of OR logic gate based on dual-aptamer strategy and two chemical input signals (PrP^{Res} and Gdn-HCl) is an important step toward the design of prion diseases diagnosis systems.

Materials and Methods

Materials

Two aptamers, Apt1, NH2-CTT ACG GTG GGG CAA TT, and Apt2, Bio-GTT TTG TTA CAG TTC GTT TCT TTT CCC TGT CTT GTT TTG TTG TCT, were selected by Takemura and Bibby [26,27], respectively, and synthesized by Sangon Tech. Ltd. (Shanghai, China) without further purification. Streptavidin modified quantum dots (QDs) were purchased from Jiayuan Quantum Dot Co. Ltd. (Wuhan, China). Guanidine hydrochloride (Gdn-HCl) was commercially available from Genview (USA). Ultrapure water (18.2 MΩ, LD-50G-E Lidi Ultra Pure Waters System, Chongqing, China) was used throughout. Bovine serum albumin (BSA) and pepsin were purchased from Shanghai Biochemicals (Shanghai, China). Other commercial reagents such as sodium chloride and nickel chloride were analytical reagent grade without further purification.

Apparatus

A Hitachi F-2500 fluorescence spectrophotometer and a U-3010 spectrophotometer (both were from Hitachi, Tokyo, Japan) were used to measure the fluorescence and absorption, respectively. A J-810 spectropolarimeter (JASCO Co., Japan) was applied to obtain the circular dichroism (CD) spectra, and a KQ-100 ultrasonic processor (Kunshan Ultrasonic Instruments Factory, Jiangsu, China) was employed for the dissociation of MMPs. The fluorescence imaging was acquired with a IX81 microscope with a 10× objective (Olympus, Japan).

Coupling of MMPs with Apt1

To improving the immobilization of aptamer on MMPs, Fe$_3$O$_4$ magnetic particles were prepared according to our previous method [28] with some modifications. Firstly, Fe$_3$O$_4$ MMPs were prepared by co-precipitating divalent and trivalent ions in alkaline solution under hydrothermal conditions [29,30]. Secondly, tetra-ethyl orthosilicate (TEOS) was used to generate silica coatings on the surface of MMPs [31]. Thirdly, NH$_2$-silanization of the silica coated Fe$_3$O$_4$ MMPs were carried out by adding 0.5 ml of 3-aminopropyltriethoxysilane (APTES) to the solution and continuously stirring for 30 min. Then, the NH$_2$-silanized Fe$_3$O$_4$ MMPs were washed with ethanol for 3 times and dried completely in oven for 30 min at 110°C.

For the coupling of Apt1 to MMPs, 10 mg MMPs was incubated in 0.01 mol/L PBS (pH 7.4) containing 2.5% (v/v) glutaraldehyde (GA) at 37°C for 1 hour with gently stirring, equilibrated overnight at 37°C with 1.4 nmol NH$_2$-Apt1 after removed redundant GA, and then washed several times and finally re-suspended in 10 mL 0.01 mol/L PBS (pH 7.4). The coupling efficiency was determined by the decreased absorbance of Apt1 at 260 nm in aqueous medium (refer to Figure S1).

Purification of Recombination Human Cellular Prion Protein (PrP^C) and the Conversion of PrP^C to PrP^{Res}

PrP^C was prepared following the reference of Xiao's group and our previous publications [25,32]. Firstly, the plasmid of recombinant human prion protein (23–231) was constructed and expressed in *Escherichia coli* BL21 (DE3). For protein purification, 50 µg/mL isopropyl-d-thiogalactopyranoside was used to induce the fresh overnight culture and the cells were harvested by centrifugation after 6 hours, then sonicated in lysis buffer (50 mmol/L NaH$_2$PO$_4$, 300 mmol/L NaCl, and 10 mmol/L imidazole, pH 8.0), and denatured in 6 mol/L Gdn-HCl overnight, then purified by nickel-nitrilotriacetic acid agarose resin (Genview). The purified proteins were analyzed by SDS-polyacrylamide gel electrophoresis and CD spectra.

PrP^{Res} was prepared according to Bocharova *et al* [33]. In short, dilute the 73.8 µmol/L α-form rPrP to 22 µmol/L and incubated at 37°C for 48 hours with 3 mol/L urea, 1 mol/L Gdn-HCl, 150 mmol/L NaCl at pH 4.0 in 20 mmol/L sodium acetate buffer, then dialysis with 20 mmol/L sodium acetate buffer. The conformation of PrP^{Res} was confirmed by CD spectra (see in Ref. 25) [25].

Discrimination and Detection of PrP^{Res}

For the discrimination of PrP^{Res}, the native state solutions or denatured state solutions that were pre-treating with 4 mol/L Gdn-HCl at 83°C for 10 min were incubated with 60 µL MMPs-Apt1 and 30 µL 1.0 mg/mL BSA in 0.02 mol/L PB (pH 6.1) containing 0.2 mol/L NaCl for 30 min at room temperature. After remove abundant proteins by magnetic separation, the re-suspension were incubated with 40 µL QDs-Apt2 in 0.02 mol/L
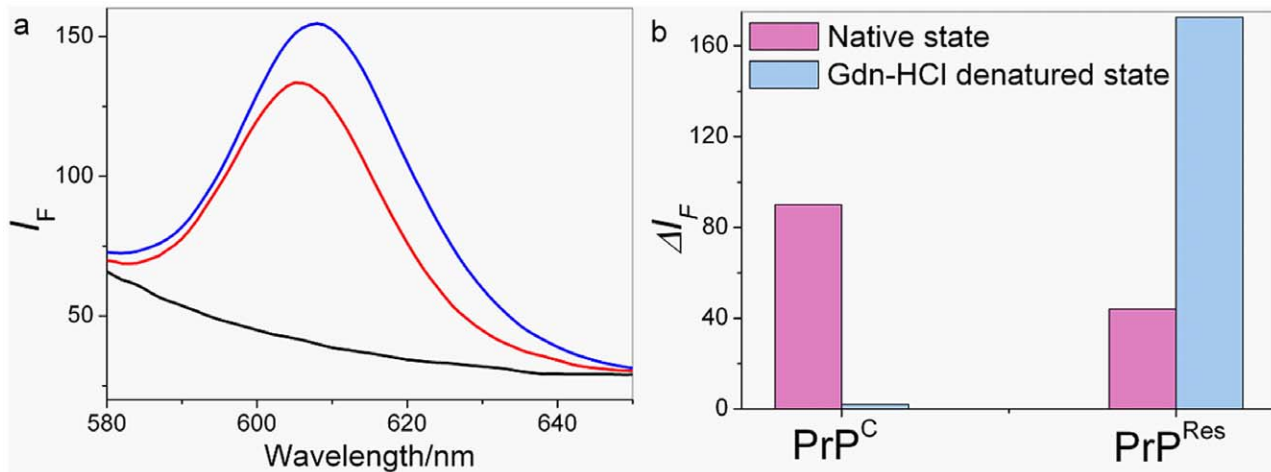
Figure 2. Fluorescence response of dual-aptamer strategy incubating with PrP. (a) The fluorescence spectra of MMPs-Apt1 and QDs-Apt2 incubated with 2.56×10^{-6} mol/L PrP^C (blue line) and 2.03×10^{-6} mol/L PrP^{Res} (red line), respectively. The black line represents control. (b) Fluorescence changes of MMPs-Apt1 and QDs-Apt2 in native state (NS) and denatured state (DS) PrP. PrP^C and DS-PrP^C, 1.52×10^{-6} mol/L; PrP^{Res} and DS-PrP^{Res}, 1.14×10^{-6} mol/L.
doi:10.1371/journal.pone.0053935.g002

PB (pH 7.4) containing 0.2 mol/L NaCl at room temperature for 60 min with end-over-end rotation. Then an external magnet was used to eliminate free QDs-Apt2. The fluorescence of Apt1-PrP-Apt2 conjugates was measured with the excitation at 365 nm and emission at 608 nm.

Figure 3. Schematic presentation (a) and the truth table (b) of dual-aptamer based logic gate. Input of i_1 (PrP^C or PrP^{Res}) for the formation of the cocktail of MMPs-Apt1-PrP-Apt2-QDs lead to an enhanced fluorescence emission (output = 1), and the input of i_2 (Gdn-HCl) leads to the fluorescence different. For PrP^{Res}, the fluorescence of the cocktail gets increased dramatically (output = 1), behaving similar to the OR logic gate, while for PrP^C, the fluorescence gets disappeared (output = 0), behaving similar to the XOR logic gate. r represents the fluorescence ratios of ($i_1 = 1$, $i_2 = 0$) or ($i_1 = 1$, $i_2 = 1$) condition to ($i_1 = 0$, $i_2 = 0$) condition.
doi:10.1371/journal.pone.0053935.g003

For PrP^{Res} detection, the samples were pretreated with 4 mol/L Gdn-HCl at 83°C for 10 min to eliminate the influence of PrP^C, and then processed the same procedure as the discrimination of PrP^{Res}.

Reuse of MMPs-Apt1 Probe

With the purpose of reusing MMPs-Apt1, the Apt1-PrP-Apt2 conjugates were incubated in 1 mol/L NaOH at 50°C for 10 min and the regenerated MMPs-Apt1 probe were collected by an external magnet.

Results and Discussion

The Principle of Dual Aptamer Strategy

Our strategy starts with the chemical modification of MMPs and QDs with Apt1 and Apt2, respectively (Figure 1). When PrP gets through the gate made up by MMPs-Apt1 and QDs-Apt2, specific recognition of the two aptamers with the corresponding epitopes of PrP occurs, which results in the formation of fluorescent cocktails of MMPs-Apt1-PrP-Apt2-QDs. As MMPs have exceptional separation ability and QDs have high photoluminescence quality, the highly fluorescent cocktails in the aqueous mediums can be separated by the outer magnetic field. It can be seen that the fluorescence intensities got increased dramatically either PrP^C or PrP^{Res} was incubated with MMPs-Apt1 and QDs-Apt2 (Figure 2a), suggesting that the two aptamers are both able to bind with PrP simultaneously and the cocktails of MMPs-Apt1-PrP-Apt2-QDs formed.

Discrimination and Detection of PrP^{Res}

It has been reported that the resistance of PrP^C and PrP^{Res} to denaturing detergents is different, PrP^C is sensitive to denaturing detergent while PrP^{Res} is partly resistant. When treated with denaturing detergent, the structure of PrP^C is destroyed while the binding epitope of 90–231 of PrP^{Res} become more accessible [34]. According to the references, the binding epitopes of Apt 1 and Apt2 correspond to the 23–90 and 90–231 amino acids of PrP, respectively [26,27]. On the basis of these, it can be assumed that PrP^{Res} could be discriminated from PrP^C based on the different affinities of the two aptamers to DS-PrP. As shown in Figure 2b,
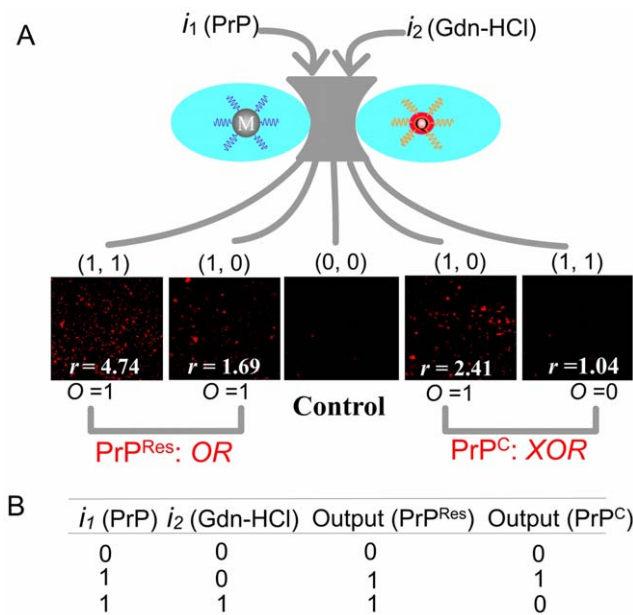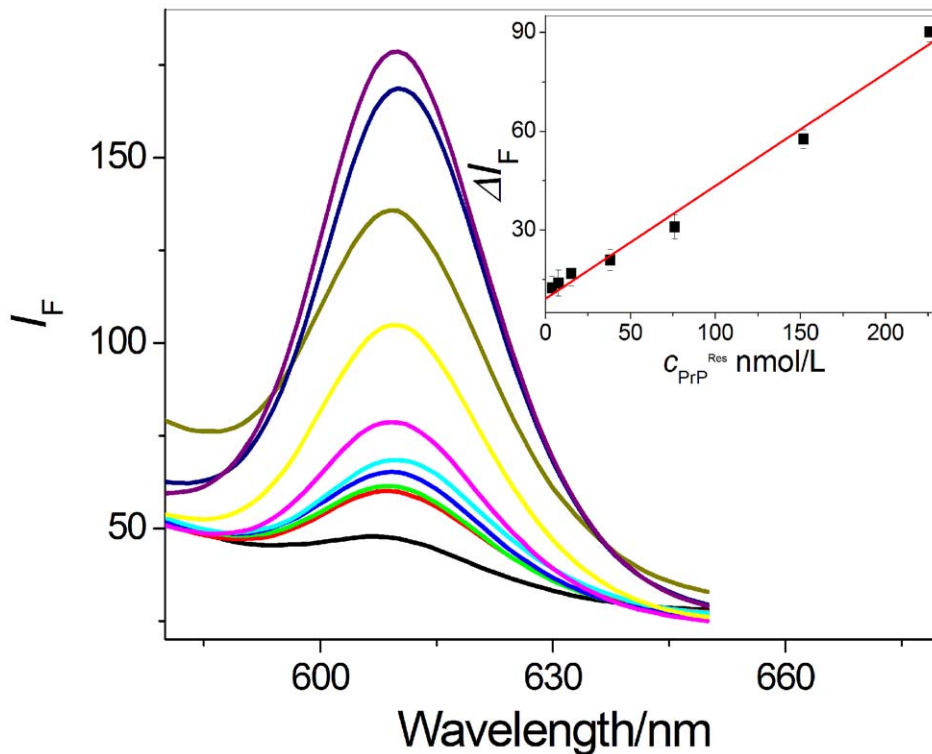
Figure 4. Detection of DS-PrP^{Res} with the dual-aptamer strategy. The linear equation is $\Delta I_F = 9.23 + 0.34\ c_{PrP}{}^{Res}$ in the range of 3.84–226.0 nmol/L with the correlation coefficient R of 0.994 (n = 7).
doi:10.1371/journal.pone.0053935.g004

MMPs-Apt1 and QDs-Apt2 bind with NS-PrP^C or NS-PrP^{Res} simultaneously with the result of forming the cocktails of MMPs-Apt1-PrP-Apt2-QDs since the two binding epitopes of native state PrP^C (NS-PrP^C) and native state PrP^{Res} (NS-PrP^{Res}) are intact, and thus high fluorescence signals could be observed easily. However, when denatured PrP (DS-PrP^C or DS-PrP^{Res}) were incubated with MMPs-Apt1 and QDs-Apt2, distinct fluorescence responses could be obtained for the reason that PrP^C and PrP^{Res} display different detergent denaturation curves [35,36]. PrP^C is sensitive to

denaturing detergent and the epitope of DS-PrP^C for Apt1 was destroyed when PrP^C was pre-treated with Gdn-HCl, therefore the cocktails can not formed with the result of non fluorescence observed. What is contrary, PrP^{Res} is resistant to Gdn-HCl and the binding epitope of DS-PrP^{Res} for Apt2 becomes more accessible after Gdn-HCl treatment, which results in the enhancement of fluorescence when MMPs-Apt1 and QDs-Apt2 incubated with DS-PrP^{Res}. These results are consistent with that of Bibby *et al* and our previous work [25,27], showing that guanidinium denatur-
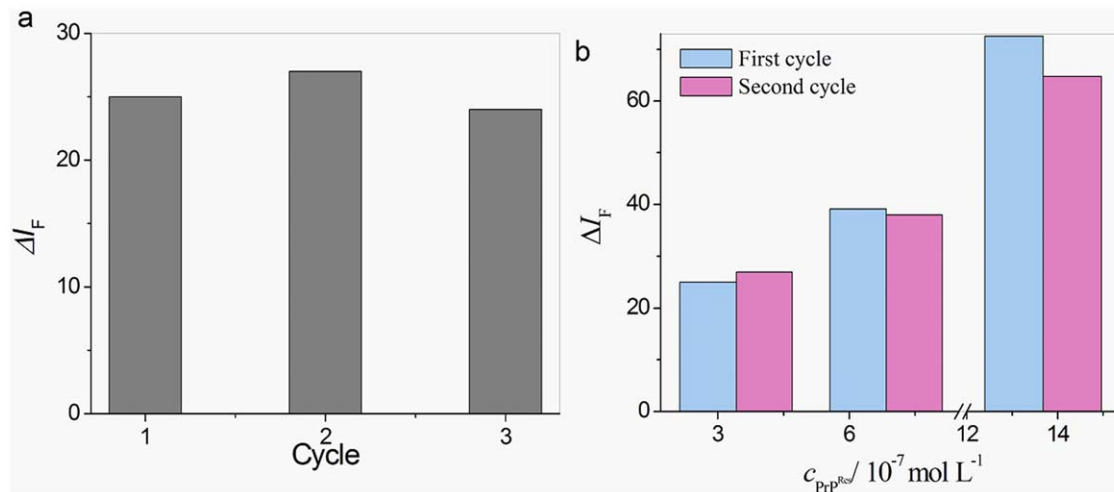

Figure 5. Reuse of MMPs-Apt1. (a) Good signal response could be achieved over three cycles. DS-PrP^{Res} concentrations was 3.42×10^{-7} mol/L. (b) The MMPs-Apt1 could be reused without loss of sensitivity in the second cycle when DS-PrP^{Res} are 3.42, 6.84, 13.86×10^{-7} mol/L.
doi:10.1371/journal.pone.0053935.g005

ation reduces the binding ability of aptamer to PrP^C and increases the binding ability of aptamer to PrP^{Res}. The strong fluorescence emission of the cocktails of MMPs-Apt1-PrP-Apt2-QDs could also be observed by a fluorescence microscope. As seen in Figure 3a, both NS-PrP^C (the 2nd picture) and NS-PrP^{Res} (the 4th picture) display strong fluorescence intensities, and DS-PrP^C (the 3rd picture) shows non-fluorescence emission while DS-PrP^{Res} (the 1st picture) displays enhanced fluorescence compared with that of NS-PrP^{Res}. The same resistance of PrP^{Res} to Gdn-HCl is similar to the results founded in the reported conformational discrimination assays [34,37,38].

In order to accomplish sensitive PrP^{Res} detection, MMPs-Apt1 and QDs-Apt2 were incubated with different content of PrP^{Res}. As seen in Figure 4, sequential increases of fluorescence emission were observed, and there is a good linear relationship between the enhanced fluorescence and the concentration of PrP^{Res} ranging from 3.84 to 226.0 nmol/L with the correlation coefficient of 0.994 (n = 7). It was found that the lowest concentration resulted in positive signal response with the present dual-aptamer strategy was 85.5 pmol/L, which is about 1000-folds lower than the detection limits of current Abs-mediated assays [9].

The Construction of Dual-Aptamer Logic Gate

In such cases, a new concept of dual-aptamer logic gate can be conceived. The new dual-aptamer logic gate have two inputs, one is PrP (i_1, PrP^C or PrP^{Res}) and the other is Gdn-HCl (i_2), and one fluorescence ratio (r) output which represents the fluorescence intensities of $i_1 = 1$, $i_2 = 0$ condition or $i_1 = 1$, $i_2 = 1$ condition to that of $i_1 = 0$, $i_2 = 0$ condition ($r = I_{(i1 = 1, \, i2 = 0)}$ or $I_{(i1 = 1, \, i2 = 1)}$ / $I_{(i1 = 0, \, i2 = 0)}$). The output is considered to be 0 when r is lower than 1.10, whereas an output is interpreted as 1 when r is higher than 1.50. It should be noted that the two thresholds level must be applied to define a forbidden range in conventional electronic gates, and any output falling between the two values is considered as an invalid result of a logic operation [39].

As a proof-of-concept for the dual-aptamer logic gate, the fluorescence responses of PrP^{Res} can be readily exploited in the design of an OR logic gate. The fluorescence ratio output (O) obtained by PrP^{Res} ($i1$) and Gdn-HCl ($i2$) as inputs are shown in Figure 3a. When $i1$ and $i2$ are equal to 0 (i.e. no PrP^{Res} and Gdn-HCl, 0–0), the fluorescence ratio r was calculated ($r = 1.0$) and $O = 0$. When PrP^{Res} was input (1–0), the fluorescence ratio r was calculated ($r = 1.69$) and $O = 1$. However, if PrP^{Res} and Gdn-HCl simultaneously get through the gate made of MMPs-Apt1 and QDs-Apt2 (i.e. PrP^{Res} and Gdn-HCl, 1–1), the fluorescence significantly increased and the fluorescence ratio $r = 4.74$ ($O = 1$). The truth table matches that for the OR gate, as shown in Figure 3b. On the contrary, PrP^C displays different Gdn-HCl denaturation curve, as shown in Figure 2b, and thus the fluorescence responses are different from those of PrP^{Res}. It can be seen in Figure 2b, the fluorescence ratio $r = 2.41$ and $O = 1$ when PrP^C was input (1–0). However, the fluorescence ratio $r = 1.04$ and $O = 1$ if PrP^C and Gdn-HCl simultaneously get through the gate (i.e. PrP^C and Gdn-HCl, 1–1), which is in accordance with XOR gate behavior.

Reuse of MMPs-Apt1 Probe

It can be seen that the sensitivity of MMPs-Apt1 could be preserved even over three cycles (Figure 5a), and the results were accordance with those of our previous work [25]. The reason might be that only a surface-tethered monolayer of Apt1 was involved in the modification of MMPs surfaces. Then the reuse of MMPs-Apt1 under different PrP^{Res} concentrations were discussed, as seen in Figure 5b, the fluorescence emission intensities in the

second cycle were similar to those in the first cycle, which suggest that the MMPs-Apt1 probe could be reused without loss of sensitivity in the second cycle. It can also be found that the fluorescence intensities under higher concentration in the second cycle were decreased compared with those in the first cycle, and the reasons were still being explored. The dissociation of PrP and MMPs-Apt1 could also be observed from the increasing fluorescence of the aqueous medium separated by magnetic field (Figure S2). Moreover, it was found that small peaks around 608 nm were observed from the suspension of reused MMPs-Apt1 probe (refer to Figure S3), and two possibilities might account for this phenomenon. The first one might be the incomplete dissociation of PrP from the MMPs-Apt1 surface, which can be avoided by further addition of NaOH. Since NaOH denaturation involved not only in PrP but also in the blocking agent of BSA, the nonspecific absorption of QDs-Apt2 on the surface of MMPs-Apt1 might be the other reason.

Conclusion

In summary, OR and XOR logic gates based on two inputs (PrP and Gdn-HCl) and a fluorescence output were demonstrated taking the advantages of exceptional separation ability of MMPs, high photoluminescence quality of QDs, and the unusual sensitivity and selectivity of dual-aptamer strategy. The two aptamers provide a way for inputs and output of individual element to link each other in the dual-aptamer design. In contrast to all previously reported aptamer-based systems, the present dual-aptamer logic gate possesses the following advantages. Firstly, the dual-aptamer strategy achieved sensitive and selective PrP^{Res} discriminating, and dual-aptamer logic gate further simplifies the result of detection, leaving the detection of PrP^{Res} either "Yes" or "No". Secondly, the inputs (PrP and Gdn-HCl) and gates (MMPs-Apt1 and QDs-Apt2) used here are all cost-saving and chemical stable molecules, which are crucial for the development of smaller, more effective molecular-scaled computers [4]. Thirdly, the MMPs-Apt1 probe could be reused without loss of sensitivity over three cycles under different concentrations. These findings should give helpful insights for the development of new dual-aptamer based device for prion diseases diagnosis at pre-symptomatic stage. To achieve this goal, further work should mainly be concentrated on the improvement of sensitivity, which might come true in virtue of the following strategies. The first one is to amplify the existing signal, for example, mass spectrometry might be used for the detection of Cd^{2+} concentration from QDs-Apt2. The other one is to concentrate the minute quantities of PrP^{Res} in samples by the exceptional separation ability of MMPs-Apt1.

Supporting Information

Figure S1 The absorption spectrum of Apt1 control (blank line) and the aqueous medium of MMPs-Apt1 after separated by external magnet (red line).
(TIF)

Figure S2 Fluorescence spectra of the supernatant of the cocktail of MMPs-Apt1-PrP-Apt2-QDs separated by magnetic field. PrP^{Res}: 0.00, 3.42, 6.84, 13.86×10^{-7} mol/L from the bottom up.
(TIF)

Figure S3 The fluorescence spectra of reused MPs-Apt1. The concentrations of DS-PrP^{Res} are corresponding to 0, 3.42, 6.84, 13.86×10^{-7} mol/L from the bottom up.
(TIF)

Author Contributions

References

1. Konry T, Walt DR (2011) Intelligent medical diagnostics via molecular logic. J Am Chem Soc 131: 13232–13233.
2. Miyoshi D, Inoue M, Sugimoto N (2006) DNA logic gates based on structural polymorphism of telomere DNA molecules responding to chemical input signals. Angew Chemie Int Ed 45: 7716–7719.
3. Benenson Y (2009) RNA-based computation in live cells. Current Opinion in Biotech 20: 471–478.
4. Chen X, Wang Y, Liu Q, Zhang Z, Fan C, et al. (2006) Construction of molecular logic gates with a DNA-cleaving deoxyribozyme. Angew Chemie Int. Ed 45: 1759–1762.
5. Margulies D, Melman G, Shanzer A (2005) Fluorescein as a model molecular calculator with reset capability. Nat Mater 4: 768–771.
6. Qu DH, Wang QC, Tian H (2005) A Half Adder Based on a Photochemically Driven [2]Rotaxane13. Angew Chem Int Ed 44, 5296–5299.
7. Silva-Rocha R, de Lorenzo V (2008) Mining logic gates in prokaryotic transcriptional regulation networks. FEBS Lett 582: 1237–1244.
8. Grassi J, Maillet S, Simon S, Morel N (2008) Progress and limits of TSE diagnostic tools. Vet. Res 39: 33.
9. Soto C (2004) Diagnosing prion diseases: needs, challenges and hopes. Nature Reviews 2: 809–819.
10. Englund H, Sehlin D, Johansson AS, Nilsson LNG, Gellerfors P, et al. (2007) Sensitive ELISA detection of amyloid-beta protofibrils in biological samples. J Neurochem 103: 334–345.
11. Coleman BM, Nisbet RM, Han S, Cappai R, Hatters DM, et al. (2009) Conformational detection of prion protein with biarsenical labeling and FlAsH fluorescence. Biochem Biophys Res Commun 380: 564–568.
12. Krafft C, Steiner G, Beleites C, Salzer R (2009) Disease recognition by infrared and Raman spectroscopy. J Biophoton 2: 13–28.
13. Fujii F, Horiuchi M, Ueno M, Sakata H, Nagao I, et al. (2007) Detection of prion protein immune complex for bovine spongiform encephalopathy diagnosis using fluorescence correlation spectroscopy and fluorescence cross-correlation spectroscopy. Anal Biochem 370: 131–141.
14. Gilch S, Schazl HM (2009) Aptamers against prion proteins and prions. Cell Mol Life Sci 66: 2445–2455.
15. Proske D, Gilch S, Wopfner F, Schatzl HM, Winnacker EL, et al. (2002) Prion-protein-specific aptamer reduces PrPSc formation. ChemBioChem 3: 717–725.
16. Weiss S, Proske D, Neumann M, Groschup MH, Kretzschmar HA, et al. (1997) RNA aptamers specifically interact with the prion protein PrP. J Virol 71: 8790–8797.
17. Huang CC, Chen CT, Shiang YC, Lin ZH, Chang HT (2009) Synthesis of Fluorescent Carbohydrate-Protected Au Nanodots for Detection of Concanav-alin A and Escherichia coli. Anal Chem 81: 875–882.
18. Zichel R, Chearwae W, Pandey GS, Golding B, Sauna ZE (2012) Aptamers as a sensitive tool to detect subtle modifications in therapeutic proteins. PLoS ONE 7: e31948.
19. Li C, Lin J, Guo Y, Zhang S (2011) A novel electrochemiluminescent reagent of cyclometalated iridium complex-based DNA biosensor and its application in cancer cell detection. Chem Commun 47: 4442–4444.
20. Goulko AA, Li F, Le XC (2009) Bioanalytical applications of aptamer and molecular-beacon probes in fluorescence-affinity assays. Trends Anal Chem 28: 878–892.
21. Chen LQ, Xiao SJ, Hu PP, Ma J, Luo LF, et al. (2012) Aptamer-Mediated Nanoparticle-Based Protein Labeling Platform for Intracellular Imaging and Tracking Endocytosis Dynamics. Anal Chem, 84: 3099–3110.
22. Chen LQ, Xiao SJ, Peng L, Wu T, Ling J, et al. (2010) Aptamer-adapted silver nanoparticles used for intracellular protein imaging and single nanoparticle spectral analysis. J Phys Chem B 114: 3655–3659.
23. Heyduk E, Heyduk T (2005) Nucleic acid-based fluorescence sensors for detecting proteins. Anal Chem 77: 1147–1156.
24. Zhang YL, Huang Y, Jiang JH, Shen GL, Yu RQ (2007) Electrochemical aptasensor based on proximity-dependent surface hybridization assay for single-step, reusable, sensitive protein detection. J Am Chem Soc 129: 15448–15449.
25. Xiao SJ, Hu PP, Wu XD, Zou YL, Ling J, et al. (2010) Sensitive discrimination and detection of prion disease-associated isoform with a dual-aptamer strategy by developing a sandwich structure of magnetic microparticles and quantum Dots. Anal Chem 82: 9736–9742.
26. Takemura K, Wang P, Vorberg I, Surewicz W, Priola SA, et al. (2006) DNA aptamers that bind to PrPC and Not PrPScshow sequence and structure specificity. Exp Biol Med 231: 204–214.
27. Bibby DF, Gill AC, Kirby L, Farquhar CF, Bruce ME, et al. (2010) Application of a novel in vitro selection technique to isolate and characterise high affinity DNA aptamers binding mammalian prion proteins. J Virol Meth 151: 107–115.
28. Hu P, Huang CZ, Li YF, Ling J, Liu YL, et al. (2008) Magnetic particle-based sandwich sensor with DNA-modified carbon nanotubes as recognition elements for detection of DNA hybridization. Anal Chem 80: 1819–1823.
29. Koneracká M, Kopčanský P, Antalík M, Timko M, Ramchand CN, et al. (1999) Immobilization of proteins and enzymes to fine magnetic particles. J Magn Magn Mater 201: 427–430.
30. Liu ZL, Liu YJ, Yao KL, Ding ZH, Wang J, et al. (2002) Synthesis and magnetic properties of Fe3O4 nanoparticles. J Mater Synth Process 10: 83–87.
31. Deng Y, Qi D, Deng C, Zhang X, Zhao D (2008) Superparamagnetic high-magnetization microspheres with an Fe3O4@SiO2 core and perpendicularly aligned Mesoporous SiO2 shell for removal of microcystins. J Am Chem Soc 130: 28–29.
32. Yu SL, Lei J, Sy MS, Mei FH, Kang SL, et al. (2004) Polymorphisms of the PRNP gene in chinese populations and the identification of a novel insertion mutation. Eur J Hum Genet 12: 867–870.
33. Bocharova OV, Breydo L, Parfenov AS, Salnikov VV, Baskakov IV (2005) In vitro conversion of full-length mammalian prion protein produces amyloid Form with physical properties of PrPSc. J Mol Biol 346: 645–659.
34. Novitskaya V, Makarava N, Bellon A, Bocharova OV, Bronstein IB, et al. (2006) Probing the conformation of the prion protein within a single amyloid fibril using a novel immunoconformational assay. J Biol Chem 281: 15536–15545.
35. Chang B, Miller MW, Bulgin MS, Sorenson-Melson S, Balachandran A, et al. (2008) PrP antibody binding-induced epitope modulation evokes immunocoo-perativity. J Neuroimmunol 205: 94–100.
36. Leliveld SR, Korth C (2007) The use of conformation-specific ligands and assays to dissect the molecular mechanisms of neurodegenerative diseases. J Neurosci Res 85: 2285–2297.
37. Peretz D, Williamson RA, Matsunaga Y, Serban H, Pinilla C, et al. (1997) A conformational transition at the N terminus of the prion protein features in formation of the scrapie isoform. J Mol Biol 273: 614–622.
38. Sun Y, Breydo L, Makarava N, Yang Q, Bocharova OV, et al. (2007) Site-specific Conformational Studies of Prion Protein (PrP) Amyloid fibrils revealed two cooperative folding domains within amyloid structure. J Biol Chem 282: 9090–9097.
39. Deonarine AS, Clark SM, Konermann L (2003) Implementation of a multifunctional logic gate based on folding/unfolding transitions of a protein. Future Gener Comp Syst 19: 87–97.